

Transient hot-phonon-to-exciton spectroscopy in organic molecular semiconductors

F. Cordella, R. Orru, M. A. Loi, A. Mura, and G. Bongiovanni

Dipartimento di Fisica, Università di Cagliari, I-09042 Monserrato and Istituto Nazionale per la Fisica della Materia, Italy

(Received 16 May 2003; published 24 September 2003)

The interaction dynamics between excitons and intramolecular vibrations is investigated in α -sexithiophene crystals using transient pump-probe spectroscopy. The ultrafast fission of vibrons, i.e., exciton states bound to intramolecular vibrations, predicted in the 1960s by Davydov and Rashba, is observed. The fission process is monitored by stimulating the optical transitions from the outgoing scattered states, the hot ground state C-C stretching vibrations, to the lowest exciton bands. The vibrational energy is dissipated in 1.5 ± 0.3 ps.

DOI: 10.1103/PhysRevB.68.113203

PACS number(s): 78.47.+p, 63.20.Kr, 78.66.Qn

After electrical or optical injection, charged or neutral excitations relax towards lower lying states, where they can accomplish two important functions: to recombine with the emission of one photon, or to contribute to charge transport. The initial excess energy is released to the lattice through a sequence of inelastic scattering events in which optical and acoustical phonons are emitted. The dynamics of carrier energy loss and the involved electron-phonon scattering mechanisms have been investigated in great detail in conventional semiconductors,¹ but to a much lesser extent in π -conjugated polymers and molecular materials. The latter have justly come into the electronic and optoelectronic world thanks to the impressive progress in new device fabrication and performances.² Energy relaxation in organic semiconductors ends up with the generation of various types of states: singlet or triplet excitons, charge transfer states, and polarons featuring quite different transport and light emission properties. The understanding of those processes which determine the relative abundance of each final state is an important challenge for device optimization. Thermalization through phonon scattering can compete with or favor interconversion between excitations.^{3,4} Its relevance to the intrinsic field-assisted dissociation of hot excitons in polymers has been also suggested.⁵ However, a detailed comprehension of the peculiar scattering processes that allow for excited-state energy loss in organics is still missing.

In this Brief Report, we investigate this issue in sexithiophene crystals. Beside its technological importance,⁶ the great deal of information available on this material⁷ and the considerable advances in sample quality make it the ideal laboratory to understand the dynamics of exciton-phonon interaction. Photoexcitations in organic systems are a complex combination of electronic excitations and intramolecular vibrations. The exciton and intramolecular phonons produced upon absorption of a quantum of light interact each other via the vibronic interaction. This coupling can give rise to bound states, called molecular *vibrons*.⁸ These hybrid particles are the “solid state” counterpart of the electron-vibrational excitations in a single molecule. Vibrons can be unstable and dissociate into unbound internal phonons and excitons, as outlined in the basic theory of electronic states of molecular solids, developed by Davydov and Rashba.⁸ The fission process is schematically shown in Fig. 1(a). In the initial vibron state, the nuclei oscillate in the excited state potential sur-

face. After fission, the outgoing electronic excitations move away, leaving the hot vibrations to oscillate in the electronic ground state configuration.

Here, we report the experimental observation of vibron fission in sexithiophene single crystals. In the experiment, short pump pulses create high energy vibrons, made up of excitons bound to four C-C stretching phonons. Vibrons decay in a very short time (< 100 fs). The resulting nonequi-

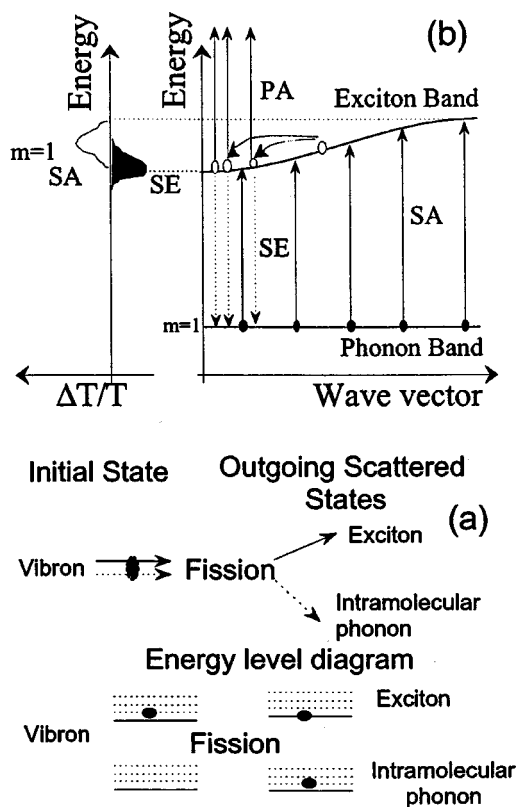


FIG. 1. (a) Fission of molecular vibrons. Initial state: a vibron made up by an exciton bound to an intramolecular phonon. Outgoing scattered states: a ground state intramolecular vibration plus a pure exciton state. (b) Survey of the optical processes stimulated by a weak probe beam with photon energy just below the optical gap. SE: exciton-to-phonon stimulated emission. SA: hot-phonon-to-exciton stimulated absorption. m : number of intramolecular phonons involved in SE and SA. PA: photoinduced absorption from the exciton band to higher energy states. $\Delta T/T$: differential transmission.

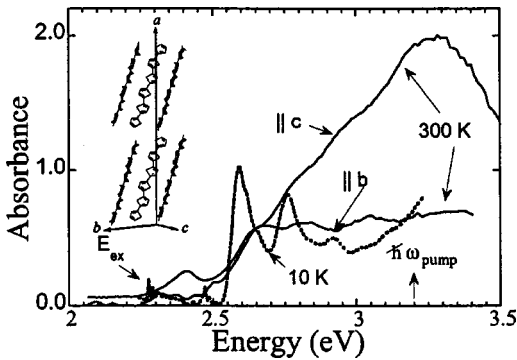


FIG. 2. Inset: unit cell of sexithiophene crystal. cw-absorbance spectra for **b**- and **c**-polarized light. Sample thicknesses for the **b**- and **c**-polarized spectra are $2.8 \mu\text{m}$ and $\ll 1 \mu\text{m}$, respectively. E_{ex} is the lowest exciton transition.

librium population of ground state C-C stretching vibrations is interrogated by a delayed probe beam. The optical process is exemplified in Fig. 1(b). Stimulated absorption (SA) from the first, second, and third vibrational quantum levels is observed. By a suitable polarization of the pump photons, excitations with a different degrees of vibronic coupling are generated. For a weak vibronic interaction, we find that only the first vibrational level is populated.

Single sexithiophene crystals were excited by the second harmonic of a regenerative amplifier Ti:Sa laser, delivering a 1-KHz train of 150-fs-long pulses at 1.61 eV. The excess photon energy ΔE with respect to the optical gap was ~ 1 eV. The excitation intensity was kept between 40 and 150 nJ/pulse, focused on a spot diameter of $80 \mu\text{m}$. Samples were held in a nitrogen atmosphere to reduce photodegradation effects. A small fraction of the infrared pump laser was focused with a suitable time delay on a 1-mm-thick sapphire plate to generate a single filament of a stable white-light continuum, which was used as the probe beam. Off-axis mirrors were used for collecting and focusing light. For probe energies below 1.8 eV, instabilities were too large to allow for reliable differential transmission ($\Delta T/T$) signals. Time-resolved photoluminescence (PL) experiments were also performed using up-conversion techniques.⁴ The comparison between PL and $\Delta T/T$ data allows us to univocally distinguish between stimulated emission (SE) and SA signals in the $\Delta T/T$ spectra. Time resolved experiments were performed at room temperature. In the following, $\Delta T/T = (T_0 - T)/T$, where T and T_0 are the probe transmission signals with and without the pump, respectively.

The unit cell and the absorbance spectra of the sexithiophene crystals are reported in Fig. 2.⁷ Single crystals have the shape of thin plates with the **b** and **c** axes in the basal plane. The lowest molecular optical transition gives rise in the crystal to several bands between 2.28 and ≈ 3.5 eV.⁹ The most intense absorption and emission resonances are observed for light parallel to the **c** axis.¹⁰ The lowest energy excitonic transition at 2.28 eV is quite weak, and is **b** polarized.⁹ The linewidth at low temperature is a few meV, revealing a negligible disorder-induced inhomogeneous broadening. The high crystal quality is fully confirmed by the absence of any significant Stokes shift between the intrinsic

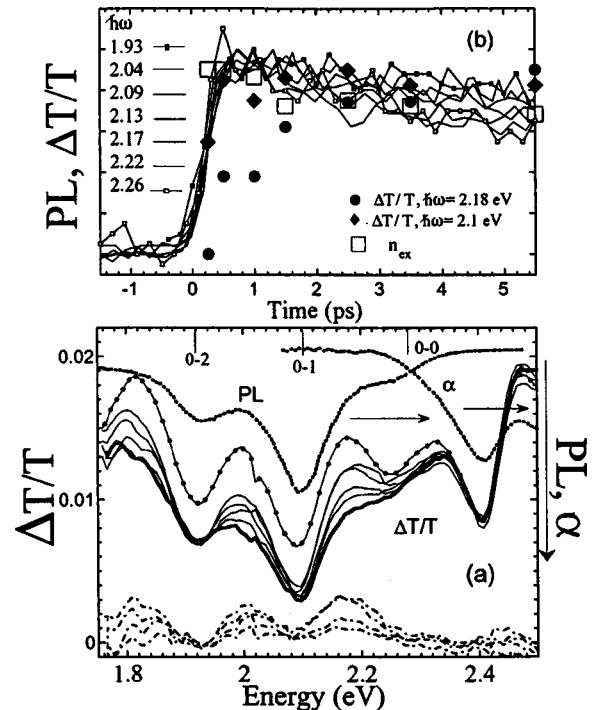


FIG. 3. (a) Dashed curves: photoluminescence (PL) and absorbance (α) spectra for **c**-polarized light. Continuous lines: differential transmission spectra ($\Delta T/T$) for different pump-probe delays. Pump and probe beams are polarized parallel to the **b** and **c** axes, respectively. Dot-dashed lines: net transient hot-phonon-to-exciton induced absorption bands, as explained in the text. The time delays Δt from the bottom to the top, are 5.5 (thick line), 2.5, 1.5, 1.0, 0.5, and 0.25 (curves with dots) ps. (b) Continuous curves: PL transients measured at different emission energies $\hbar\omega$. Diamonds and circles are the transients of $-\Delta T/T$, reported in panel (a), at 2.1 and 2.18 eV, calculated using an offset value of 0.014. Squares represent the renormalization factor n_{ex} , proportional to the exciton density.

b-polarized pure excitonic emission and absorption.^{4,10,11} On these bases, the observation in time resolved experiments of disorder-induced relaxation kinetics, like exciton spectral diffusion within an inhomogeneously broadened density of states,¹² is excluded.

The upper part of Fig. 3(a) shows the **c**-polarized PL and the **c**-polarized absorbance (α) in the spectral range between 2.1 and 2.5 eV. These spectroscopic data allow us to identify the exciton and vibronic transitions probed in the $\Delta T/T$ experiments. The low energy part of the absorption spectrum is dominated by transitions to a set of vibron states, yielding the composite structure at 2.4 eV.⁹ The PL consists of a vibronic progression in which a free exciton is annihilated and $m \neq 0$ quanta of the C-C stretching mode, $\hbar\omega_{CC} = 0.18$ eV, are created. As shown in Ref. 10, for **c**-polarized light, the pure excitonic transition is forbidden, while the vibronic replica are dipole allowed. The weak shoulder at ~ 2.25 eV is omnipresent in photoluminescence spectra of crystalline sexithiophene,¹¹ and is assigned to the emission of a low energy vibration.

The **c**-polarized PL spectrum is two order of magnitude more intense than the **b**-polarized one.¹⁰ As a similar polar-

ization ratio is expected for hot-phonon-to-exciton transitions, the $\Delta T/T$ experiments were done with a c-polarized probe beam, while both pump polarizations were used. We first discuss experiments with the electric field of the exciting laser directed along the **b** axis. $\Delta T/T$ spectra are reported in Fig. 3(a) for various delays Δt between the pump and probe beams. The $\Delta T/T$ curves are suitably renormalized, as described in more detail later on, to account for a small reduction, $\sim 20\%$, of the exciton population. A few picoseconds after excitation, the spectral shape of the nonlinear transmission, shown through a thick line in Fig. 3, becomes independent of delay. The observed structures match those in the PL and α spectra very well. We thus correlate the peak at 2.4 eV with the bleaching of the vibronic transitions.¹³ The structures at energies lower than the forbidden pure excitonic transition at 2.28 eV are assigned to SE from the bottom of the exciton band to the m -vibrational levels of the electronic ground state. A net optical gain is not observed, owing to the simultaneous presence of an intense photoinduced absorption (PA). This signal has been attributed to transitions from the lowest exciton level to higher excited states.¹⁴ However, the very similar shapes of the SE and PL spectra indicate that the PA response in the spectral range 1.8–2.4 eV is smooth.

The amplitudes of the SE, bleaching, and PA show a decrease of $\sim 20\%$ for increasing Δt . To facilitate a comparative spectral analysis at different delays, the $\Delta T/T$ curves in Fig. 3(a) represent the original experimental spectra vertically shifted and divided by a factor n_{ex} , in order to get the same bleaching response observed for $\Delta t = 0.25$ ps at 2.4 eV. The $\Delta T/T$ spectrum at $\Delta t = 0.25$ ps is reported without any data processing. As both the bleaching and SE are proportional to the photoexcitation population, the scaling procedure counterbalances the effect of exciton decay on the $\Delta T/T$ response.¹⁵ In Fig. 3(b), the values of n_{ex} , which result from the $\Delta T/T$ renormalization at different delays, are compared with the PL transients. The latter directly monitor the exciton population dynamics. The good agreement between PL and n_{ex} decays provides an independent experimental support to the validity of the $\Delta T/T$ scaling procedure.

SE and PL reach maximum values after a delay $\tau_r \sim 0.3 - 0.4$ ps. This early $\Delta T/T$ dynamics monitors the fast relaxation of excitons towards the lowest energy band. The present estimate of τ_r is in good agreement with recent reports.^{14,16} For $\Delta t > \tau_r$, $\Delta T/T$ still shows pronounced SA bands, which last a few picoseconds, at the high-energy side of each of the vibronic emission lines. To isolate this contribution, the spectrum taken at a long delay, $\Delta t = 5.5$ ps, when SA is negligible, has been subtracted from all the differential transmission curves. The resulting curves are shown in the bottom part of Fig. 3; they feature peaks at 2.18, 2.00, and 1.82 eV. We assign these structures to transitions from the hot $m = 1, 2, 3$ quantum vibrations of the ground state C-C stretching mode to the lowest exciton band. Transitions from the $m = 4$ vibrational levels might be also active, but their frequency is too close to the IR pump energy to be detected. Typically, SA is expected, as shown in Fig. 1(b), at higher energies with respect to SE, since intramolecular phonons are spread over all the Brillouin zone, due to their flat energy dispersion, while excitons mainly occupy states with a low

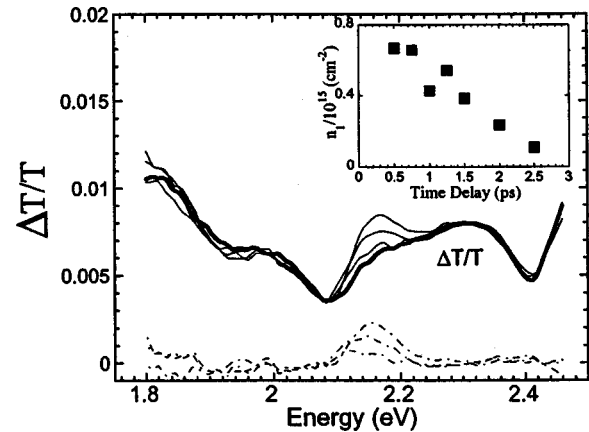


FIG. 4. Differential transmission spectra ($\Delta T/T$) for different pump-probe delays. Pump and probe photons are c polarized. Dot-dashed lines: Net transient hot-phonon-to-exciton induced absorption bands, as explained in the text. The time delays Δt from the bottom to the top, are: 5 (thick line), 2.5, 1.5, and 0.5 ps. Inset: hot phonon density n_1 vs time delay.

wave vector.⁸ Such a correlation between SE and SA spectra has been verified in polyacene crystals,¹⁷ where SA from thermally excited low frequency vibrations has been observed.

In the following, we discuss if a slow thermalization towards the low energy exciton states can provide an alternative explanation to the $\Delta T/T$ behavior for $\Delta t > \tau_r$. The delayed filling of the bottom exciton states must give rise to slower SE contributions at the low energy side of each SE band,¹² which may then explain the retarded vibronic transients at 2.18, 2.00, and 1.82 eV. The hot relaxation model is, however, ruled out on the following bases: (1) A slow exciton cooling implies that *all* the SE vibronic transitions from the hot exciton band must have a delayed, low energy contribution. Conversely, Fig. 4 shows that only one of the three vibronic SE satellites features a slow component for c-polarized pump excitation. (2) Any delayed SE signal must be also observed as delayed emission in PL. Figure 3(b) shows the transient PL emissions for energies spanning the vibronic bands. The absence of any retarded emission conclusively implies that the $\Delta T/T$ response is not due to a slowly rising SE, but to a slowly decaying SA.

We show in this paragraph that the observation of hot $m = 1, 2$, and 3 quantum vibrational levels of the ground state C-C stretching mode is consistent with the energy level scheme of sexithiophene. The major contribution to the **b**-polarized absorption spectrum is provided by the vibron progression with origin at 2.6 eV shown in Fig. 2.^{9,18} In the $\Delta T/T$ experiments, the pump photon energy is just below the $n = 4$ vibronic replica. This vibron state is made up by an exciton bound to $m = 4$ C-C stretching internal phonons. The fission decay pathways are several: the vibron can dissociate into m ground state vibrational quanta, with m between 1 to 4, plus one molecular vibron, formed by an exciton bound to $4 - m$ intramolecular phonons. The rate of the m -SA transition scales as $n_m I(m)$, where n_m is the density molecules in the m -vibrational quantum level, and $I(m)$ is the Franck-Condon factor. All the SA bands exhibit the same intensity;

hence $n_m \propto I_m^{-1}$. As I_m decreases for increasing m , we conclude that vibron fission preferentially yields hot ground state vibrations with high m values.

A further support to the vibron fission theory comes from the dependence of $\Delta T/T$ on the pump polarization. Figure 2 shows that **c**-polarized pump photons excite the strongly allowed ($m=0$) b_u exciton-polariton band at 3.3 eV.⁹ This electronic level, characterized by a vanishing vibronic interaction, retains the same equilibrium nuclear position of the ground state. We therefore expect that energy relaxation involves the C-C stretching mode to a much lesser extent. $\Delta T/T$ data for the **c**-polarized pump beam are shown in Fig. 4. Spectra are renormalized as in Fig. 3. Only the $m=1$ vibrational sublevels of the electronic ground state are populated. Intermediate vibron bands, characterized by a stronger vibronic coupling,⁴ are excited during energy relaxation.

These states are responsible for the generation of the hot unbound C-C stretching phonons.

Finally, hot-phonon-to-exciton spectroscopy allows us to measure the phonon population lifetime, a physical quantity not directly accessible via coherent experimental techniques. The inset of Fig. 4 reports the phonon population n_1 , as a function of the pump-probe delay. n_1 has been estimated as $n_{ex}SA(1)/SE(1)$, where $SA(1)$ and $SE(1)$ are the intensities of the $m=1$ SA and SE bands, and n_{ex} is the absolute exciton density. The exponential fit to the decay data gives $\tau = 1.5 \pm 0.3$ ps. τ is longer than the phonon dephasing time,¹⁶ indicating that elastic phonon-phonon scattering processes are the dominant ones.

In conclusion, we have reported the experimental observation of vibron fission in molecular crystals. This microscopic process represents a basic mechanism of excited state energy relaxation in organics.⁸

¹ *Ultrafast Spectroscopy of Semiconductors and Nanostructures*, edited by J. Shah (Springer, Milan, 1996).

² R. H. Friend *et al.*, *Nature (London)* **397**, 121 (1999).

³ G. Lanzani *et al.*, *Phys. Rev. Lett.* **87**, 187402 (2001).

⁴ M. A. Loi *et al.*, *Phys. Rev. Lett.* **86**, 732 (2001).

⁵ V. I. Arkhipov *et al.*, *Phys. Rev. Lett.* **82**, 1321 (1999).

⁶ See, e.g., F. Garnier *et al.*, *Science* **265**, 1684 (1994); *Appl. Phys. Lett.* **72**, 2087 (1998); G. Gigli *et al.*, *ibid.* **75**, 439 (1999).

⁷ See, e.g., C. Taliani *et al.*, in *Semiconducting Polymers: Chemistry, Physics, and Engineering*, edited by G. Hadziioannou and P. F. van Hutten (Wiley, New York, 2000).

⁸ A.S. Davydov, *Theory of Molecular Excitons*, (McGraw-Hill, New York, 1962); A. S. Davydov and A. A. Serikov, *Phys. Status Solidi* **42**, 603 (1970) *ibid.* **44**, 127 (1971), V. L. Broude, E. I. Rashbe, and E. F. Sheka, *Spectroscopy of Molecular Excitons* (Springer, Berlin, 1983); G. Fischer, *Vibronic Coupling* (Academic Press, London, 1984).

⁹ M. A. Loi *et al.*, *Phys. Rev. B* **66**, 113102 (2002).

¹⁰ F. Meinardi *et al.*, *Phys. Rev. Lett.* **89**, 157403 (2002).

¹¹ M. Muccini *et al.*, *J. Chem. Phys.* **108**, 7327 (1998).

¹² R. Kersting *et al.*, *Phys. Rev. Lett.* **70**, 3820 (1993).

¹³ As the vibron satellite at 2.4 eV is made up by an exciton bound to one vibration, the occupation of the lowest exciton band also bleaches the vibron transition owing to phase-space filling effects (Ref. 1).

¹⁴ S. V. Frolov *et al.*, *Phys. Rev. B* **63**, 205203 (2001). We observe a net optical as reported by Frolov *et al.*, when the probe beam is not perpendicular to the sample. With increasing tilting angle, but with the beam always *c* polarized, SE increases and PA decreases, suggesting a different orientation of the corresponding transition dipoles.

¹⁵ C. Gadermaier *et al.*, *Phys. Rev. Lett.* **89**, 117402 (2002).

¹⁶ G. Cerullo *et al.*, *Phys. Rev. Lett.* **83**, 231 (1999).

¹⁷ S. D. Colson *et al.*, *J. Chem. Phys.* **48**, 2215 (1968).

¹⁸ M. Andrzejak *et al.*, *J. Chem. Phys.* **117**, 1328 (2002).